

PLASMA POLYMERIZATION IN HEXAMETHYLDISILOXANE-ARGON
DISCHARGES PRODUCED IN A MAGNETRON SYSTEM WITH A COPPER CATHODE

T. Shiosawa, R.P. Mota*, M.C. Gonçalves⁺, J.H. Nicola e
M.A. Bica de Moraes

Instituto de Física Gleb Wataghin, UNICAMP, 13081 Campinas, SP.

* Universidade Estadual Paulista, Guaratinguetá, SP.

+ Instituto de Química, UNICAMP, 13081 Campinas, SP.

ABSTRACT

Polymer-metal composite films have been deposited in glow discharge plasmas of hexamethyldisiloxane (HMDS) and argon in a planar magnetron system with a copper cathode. Actinometric optical emission spectroscopy was used to identify the chemical species in the discharge and the trends in their concentrations as a function of the discharge parameters (total pressure of the mixture HMDS-Ar, proportion of HMDS and Ar in the gas feed and cathode voltage). The relative contributions of gas-phase reactions and cathode sputtering to the plasma composition are discussed. The structure of the films was investigated by transmission electron microscopy. Residual stress measurements were also performed in the films using the bending beam method. The correlation between the discharge parameters and the film microstructure and composition is examined.

1. INTRODUCTION

Plasma polymerization is a well established technique for the production of dielectric thin films presenting remarkable physical and chemical properties. Integrated circuit lithography [1], integrated optics [2], ultrafiltration membranes [3] and protective coatings [4] are examples of technological applications of plasma polymers.

In the last decade, plasma polymers incorporated with metals began to be studied [5]. These composite materials are prepared by a combination of the techniques of plasma polymerization and sputtering [6] or thermal evaporation [7]. Their structure is similar to that of the cermet films [8], i.e., consists of a dispersion of microscopic metallic particles embedded in the polymer matrix. This type of structure is responsible for the peculiar optical [9], electrical [10] and mechanical [11] properties of the films. Wide variations in the optical constants and electrical conductivity can be attained by varying the metal

proportion in the film. Thus, control of the process of deposition is crucial in the preparation of films with predetermined properties.

One of the successful techniques which have been used in monitoring the process of deposition of polymer-metal films is actinometric optical emission spectroscopy (AOES). This method has the advantage of being non-intrusive and is very useful in the analysis of reactive plasmas, allowing measurements on the relative changes of density of gas-phase species which contribute to film formation.

In this paper we study polymer-metal composite films produced by the codeposition of plasma polymerized hexamethyldisiloxane [HMDS, chemical formula $(CH_3)_3SiO$] and sputtered copper. Plasma polymerized HMDS presents two interesting properties which are very important in technological applications: (i) high transparency in the visible range of the spectrum, and (ii) strong adhesion to metal and dielectric substrates. The AOES technique was used to characterize the discharge while the microstructure of the films were determined by transmission electron microscopy (TEM). Residual stress measurements were also performed in order to investigate the role of intrinsic stress in the film mechanical stability.

2. BACKGROUND: ACTINOMETRY

The technique of actinometric optical emission spectroscopy, or actinometry has been proposed by Coburn and Chen [12] as a method of diagnosis of reactive plasmas. In this procedure, a small proportion of a non-reactive gas - the actinometer - is added to the feed gas in order to probe the plasma. The intensity of an optical emission line of the actinometer is given by

$$I_a = n_a \eta_a \quad (1)$$

where n is the density of ground state actinometer molecules and η_a is the

excitation efficiency from ground state to the state responsible for the emission. It should be remembered that η_a depends on the electron energy distribution function (EEDF) of the plasma and increases as the activity of the plasma is increased. The parameter "activity", A , has been defined in an earlier paper [13] as

$$A = \rho E \quad (2)$$

where ρ and E are respectively the electron density and the electron mean energy. If n is constant, which is usually the case in actinometric measurements, we can see from Eq. (1) that changes in the intensity of the actinometer emission reflect changes in the plasma activity.

Combined optical emission measurements of a reactive species, x , and that of the actinometer allows the determination of the relative changes in the density of the former as the deposition parameters (composition of the feed gases, pressure in the chamber and applied power to the plasma) are varied. Let I_x be the intensity of an emission line of species x . Then

$$I_x = n_x \eta_x \quad (3)$$

where n and η are respectively the density of the ground state reactive species and the excitation efficiency. Combining Eqs. (1) and (3) we may write

$$n_x = n_a \frac{I_x \eta_a}{I_a \eta_x} \quad (4)$$

choosing excited states of the actinometer and reactive species such that η is approximately equal or proportional to η_x , we will have, for constant n_a :

$$n_x \approx k \frac{I_x}{I_a} \quad (5)$$

where k is a constant.

3. EXPERIMENTAL

The discharges in the HMDS and Ar mixtures were generated by a homemade planar magnetron electrode connected to a negative DC power source, as represented schematically in Fig. 1. The magnetic

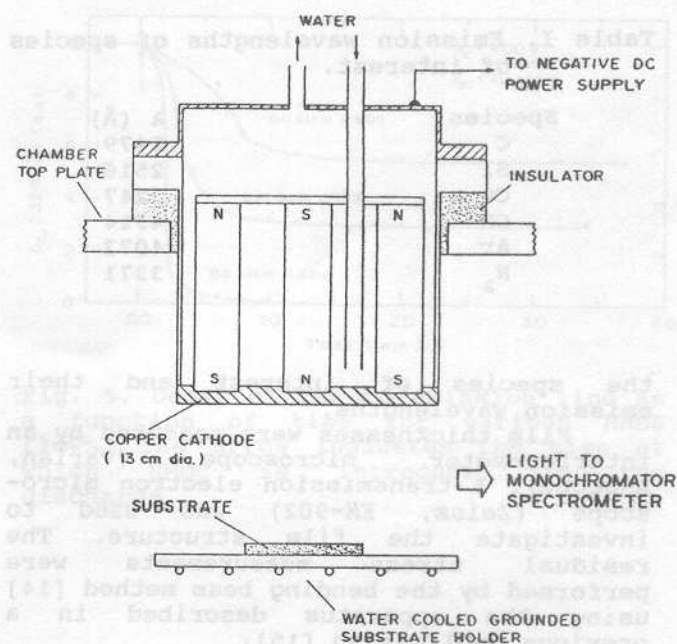


Fig. 1. Schematic diagram of the electrodes.

field in the discharge is supplied by the magnet shown in the figure, which is formed by a stack of circular loudspeaker magnets of 9 cm diameter. The electrodes were assembled inside a 30 cm diameter x 35 cm height aluminium vacuum chamber evacuated independently by a $12 \text{ m}^3 \text{ h}^{-1}$ two-stage rotary vane pump or a 150 l s^{-1} diffusion pump. Pressure in the chamber is measured by a capacitance manometer (Datametrics Barocel type 600) and by a Penning gauge (Edwards model CP-25S). Pressures during film deposition were typically in the 0.05 - 0.1 mbar range. Prior to gas admission, the chamber was pumped out to the 10^{-5} mbar range by the diffusion pump during approximately 10 minutes.

Argon, nitrogen and HMDS vapor were admitted to the chamber through mass flow controllers (Datametrics, model 825). An evaporation cell was used to produce the HMDS vapor. It consists of a 10 cm glass bulb half-filled with liquid HMDS and connected to the mass flow controller through a leak valve (Edwards, model LV-5). Both gases and HMDS are of chemical purity better than 99.9%.

A quartz glass window in the chamber allows observation of light emitted by the plasma by a 1 m focal length optical monochromator (Spex, model 14300) equipped with a photomultiplier tube (Burle, 1P20A). Optical emission spectra were recorded by a strip chart recorder (Hewlett-Packard, 7100BM). Table I lists

Table I. Emission wavelengths of species of interest.

Species	λ (Å)
C	2479
Si	2516
Cu	3247
CH	4314
Ar	4072
N ₂	3371

the species of interest and their emission wavelengths.

Film thicknesses were measured by an interferometer microscope (Varian, λ -Scope). A transmission electron microscope (Zeiss, EM-902) was used to investigate the film structure. The residual stress measurements were performed by the bending beam method [14] using the apparatus described in a previous publication [15].

4. RESULTS

4.1 Optical Emission Spectroscopy of the Discharge

Typical emission spectra of the HMDS-Ar discharge are shown in Fig. 2 in various wavelength ranges. Including Ar and N₂, which is used as an actinometer, emissions from Cu, C, CH and Si species are prominent in the discharge. While Cu arises from sputtering of the cathode, two mechanisms may account for the appearance of the C, CH and Si species: fragmentation of the HMDS molecules by the free electrons of the plasma and sputtering of the polymeric material

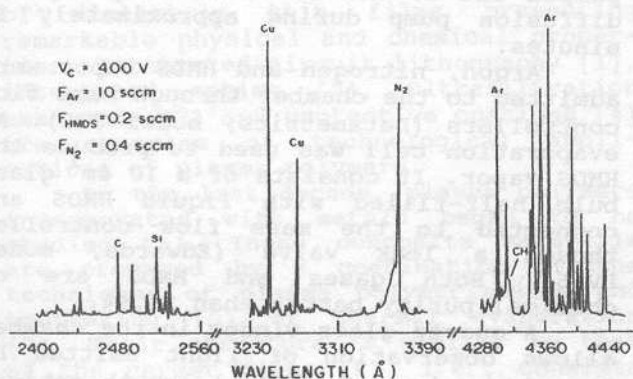


Fig. 2. Optical emission spectra of a HMDS-Ar discharge in several wavelength ranges. Nitrogen is added to the gas feed as an actinometer. The cathode voltage and the flows of Ar, HMDS and N₂ admitted to the chamber are illustrated above.

deposited on the cathode.

Figure 3 shows the intensity of emission of the actinometer (N₂) as a function of the Ar flow in a discharge without HMDS. Since the partial pressure of N₂ is nearly constant in the discharge we may conclude from the figure that the excitation efficiency for N₂ is also constant and consequently the activity of the plasma is not changed when the Ar flow varies from 10 to 14 sccm.

An entirely different behavior of the emission of N₂ is observed even when a small flow of HMDS is added to the feed gas. The dependence of the N₂ signal as a function of time, when HMDS is introduced in the discharge, is shown in Fig. 4. The steep rise in the intensity of the N₂ emission shows that the activity of the plasma is strongly increased by the presence of HMDS in the discharge. It is interesting to note that instead of levelling-off, the N₂ signal goes through a maximum and then decreases. We interpret this apparently odd behavior as due to the deposition of an insulating polymer coating on the electrodes thus reducing the discharge current. It should be mentioned however that the nature of the coating deposited on the cathode is different from that of the anode. As observed by several investigators [16] in plasma deposition in mixtures of organic gases and Ar, the polymer deposited on the cathode is a hydrogen-deficient material whose structure is deeply modified by the intensive bombardment of Ar ions.

This cathode coating also affects the flux of sputtered Cu atoms. Figure 5 shows the decays of the Cu emission lines

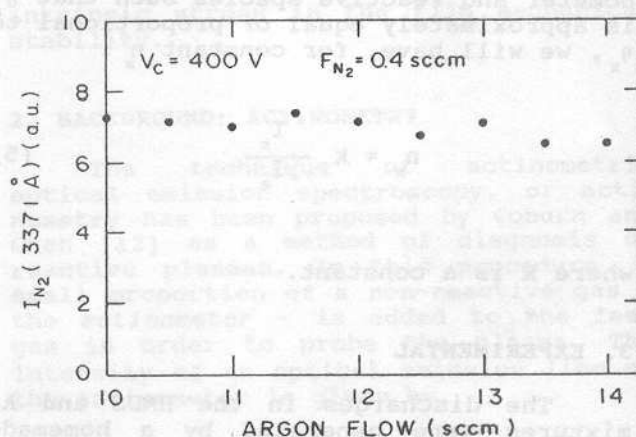


Fig. 3. Intensity of emission of N₂ as a function of the Ar flow in a discharge without HMDS.

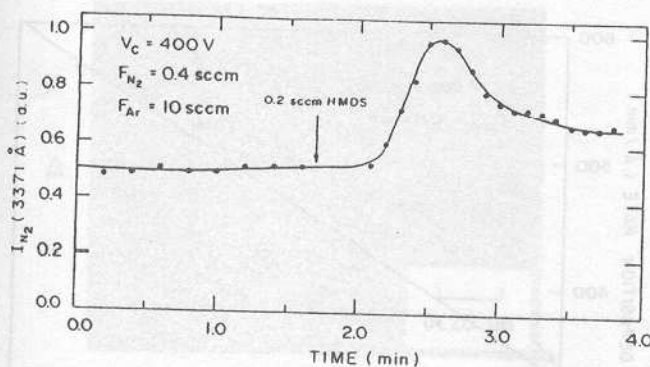


Fig. 4. Intensity of emission of N_2 as a function of time. The arrow indicates the time at which HMDS is introduced in the discharge.

with time for three different flows of HMDS. The data of each decay was taken after a thorough cathode cleaning. The intensities of the Cu signals before introducing HMDS in the discharge are normalized to unity. For the HMDS flow of 0.3 sccm, the coating is formed very rapidly on the cathode and sputtering of Cu is totally inhibited at 1.5 minutes after HMDS is introduced in the gas feed. For HMDS flows of 0.11 and 0.21 sccm the rate of formation of the coating is smaller and the emission of sputtered Cu atoms from the cathode is only partially inhibited.

The growth rate of the polymeric coating on the cathode is the difference between the rate of polymer formation and the rate of etching by Ar and other massive positive ions of the discharge. The fact that steady-state fluxes of sputtered Cu atoms are attained for the HMDS flows of 0.11 and 0.21 sccm implies that the level of contamination of the cathode surface by the polymeric layer remains constant. This means that the rates of polymer formation and etching are equal. Since the preparation of films in the anode with uniform Cu density depend on a constant Cu gas-phase concentration, the plots of Fig. 5 illustrate the usefulness of optical emission spectroscopy in monitoring the process of deposition. It should be noted also that for HMDS flows smaller than 0.3 sccm, polymer films without Cu can be formed on the anode.

Since, as shown in the spectra of Fig. 2, atomic C and atomic Si are present in the discharge, it seems interesting to investigate the mechanisms of formation of these species. As pointed out earlier, fragmentation and sputtering effects may contribute to the formation of C and Si species. In order to investigate the relative importance of

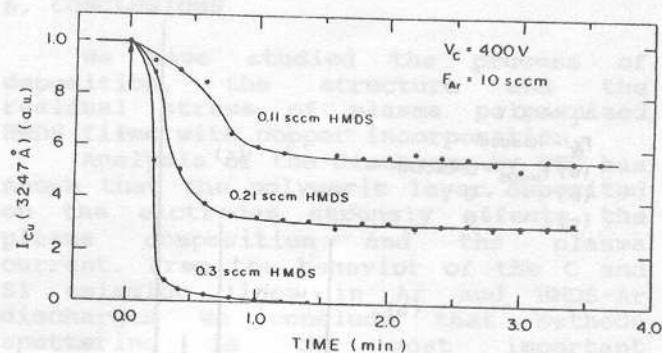


Fig. 5. Decay of the Cu emission line as a function of time for various HMDS flows. The arrow indicates the time at which HMDS is introduced in the discharge.

these two effects, we have measured the emission intensities of C and Si in Ar discharges with and without HMDS. Figure 6 shows several emission spectra of the discharge in the wavelength region between 2400 and 2560 Å. The spectrum of Fig. 6(a) was taken with HMDS in the discharge while those of Figs. 6(b) and 6(c) were taken without HMDS. The latter were taken 5 and 10 minutes after that of Fig. 6(a). As seen in the figure, the C and Si signals are clearly present in the discharge as well as the peaks at 2443 and 2492 Å and the band at 2470 Å, not yet identified. Table II lists the relative concentrations of C and Si in the discharges, calculated from the data of Fig. 6, using Eq. (5) and taking N as the actinometer. From the small changes in the densities of C and Si species in discharges with and without HMDS we conclude that sputtering plays a much more important role than fragmentation in the appearance of atomic C and Si in the plasma.

Actually the excitation efficiencies of C, Si and N corresponding to the emission lines of Table I are not similar and consequently Eq. (5) does not apply rigorously. However, due to the difficulty of finding excited states in either C or Si with excitation efficiencies similar to those of N_2 , Eq. (5) provides a first order approximation for the determination of the relative densities.

4.2 Rate of Deposition and Film Structure

The rate of deposition on the anode and the proportion of copper to polymer in the films vary widely according to the discharge parameters. Figure 7 shows the deposition rate as a function of the Ar

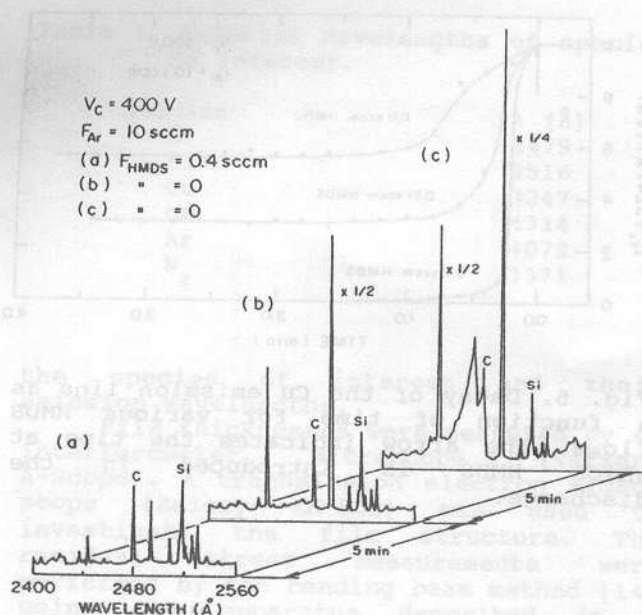


Fig. 6. Emission spectra of the discharge taken sequentially in 5 min intervals. (a) HMDS-Ar discharge. (b) and (c) Ar discharge.

flow for a constant cathode voltage and HMDS flow. The discharge parameters for the data point indicated by an arrow in the figure are the same as for the data of the uppermost curve of Fig. 5. This implies that Cu must be present in the discharge and consequently incorporated in the film. Since a rise in the Ar flow increases the flux of sputtered Cu from the cathode, films with increasing Cu content are expected to be deposited as the Ar flow changes from 10 to 14 sccm.

Transmission electron micrograph pictures of two films prepared under different conditions are shown in Fig. 8. The Ar flow varies from one sample to another while the cathode voltage and the HMDS flow are kept constant. As seen in the pictures, microscopic metallic particles (dark regions) are dispersed in the bulk of the polymer matrix. The density of metal increases from sample A to B as a consequence of the increase in

Table II. Relative densities of C and Si species in the discharge as a function of time.

Species	0 min	5 min	10 min
C	1.0	1.0	1.2
Si	1.0	0.96	0.80

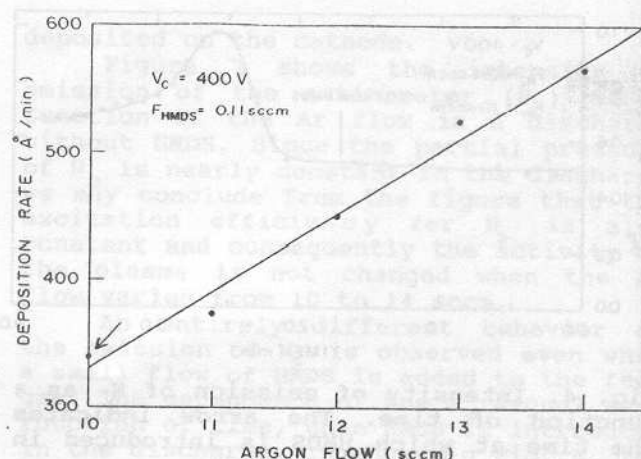


Fig. 7. Deposition rate in a HMDS-Ar discharge as a function of the Ar flow.

the Ar flow. These structures are consistent with previous observations in polymer-metal [17] and oxide-metal [18] composite films.

It should be pointed out that since atomic C and Si are present in the discharge, thus it is possible that the particles in the film are not constituted only by Cu but also contain C and Si either in metallic or combined forms such as carbides and silicides. In preliminary experiments using transmission electron diffraction we have observed that the films show well-defined diffraction rings even in samples with small Cu concentrations. It is thus expected that this technique will provide useful information on the crystalline structure of the particles.

4.3 Residual Stress Measurements

All the measurements in the films have shown that the stresses are compressive with values in the $10^8 - 10^9$ dyne cm^{-2} range. Table III lists the residual stresses of three films: a Cu-free, a polymer-Cu composite film and a polymer-free film. As previously observed [15, 19, 20], the residual stress depends on the film composition, structure and thickness. Since the thicknesses of the films listed in the table are similar, differences in stress due to thickness differences are eliminated. The all-metal film is that with the lowest stress while the composite film presents the highest stress.

Our results are different from those of Yasuda *et al.* [21] who report zero stress for plasma polymerized tetramethylsiloxane, a chemical compound

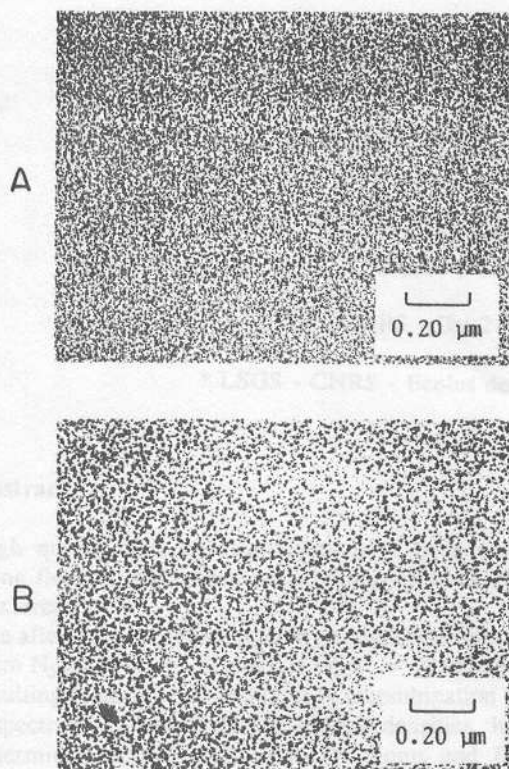


Fig. 8. TEM micrographs of two polymer-metal composite films prepared with $V = 400$ V and $F_{\text{HMDS}} = 0.15$ sccm. A: $F_{\text{Ar}} = 7.0$ sccm. B: $F_{\text{Ar}} = 10$ sccm.

very similar to HMDS.

The residual stress plays an important role in the mechanical stability of coatings. If the internal stress is too high, the internal forces in the film may overcome the adhesion forces to the substrate causing film cracking or peeling. As pointed out earlier, plasma polymerized HMDS show very good adhesion to substrates. Since our films are highly stressed, we interpret their long-term mechanical stability as a consequence of large adhesion forces between film and substrate.

Table III. Residual stress of films prepared at various HMDS and Ar flows.

Film thickness (Å)	F_{HMDS} (sccm)	F_{Ar} (sccm)	σ (dyne.cm ⁻²)
1510	0.4	0.0	1.5×10^9
1410	0.4	6.0	5.9×10^9
1580	0.0	6.0	5.0×10^8

5. CONCLUSIONS

We have studied the process of deposition, the structure and the residual stress of plasma polymerized HMDS films with copper incorporation.

Analysis of the discharge by OES has shown that the polymeric layer deposited on the electrodes strongly affects the plasma composition and the plasma current. From the behavior of the C and Si emission lines in Ar and HMDS-Ar discharges we conclude that cathode sputtering is the most important "channel" for the appearance of these species in the gas phase.

The structure of the films is typical of polymer-metal composites. The size of the metal particles increases with increasing proportions of Ar in the gas feed. Due to the presence of C and Si species in the discharge, it is possible that metallic C and Si and their compounds (carbides and silicides) are also present in the metal particles.

The long-term mechanical stability of our films, in spite of being highly stressed, strongly indicates high adhesion forces between film and substrate.

ACKNOWLEDGMENTS

We thank FAPESP, FINEP and FAEP of UNICAMP for financial support. The contribution of Dr. F. Galembeck of the Institute of Chemistry, UNICAMP, in providing the hexamethyldisiloxane used in this work is greatly appreciated.

REFERENCES

1. M. Hori, H. Yamada, T. Yoneda, S. Morita and S. Hattori, *J. Electrochem. Soc.*, 134, 707 (1987).
2. P. K. Tien, G. Smolinsky and R. J. Martin, *Appl. Opt.*, 11, 637 (1972).
3. Y. Osada and M. Takase, *J. Polym. Sci.: Polym. Chem. Ed.*, 23, 2425 (1985).
4. P. Schreiber, M. R. Wertheimer and A. M. Wrobel, *Thin Solid Films*, 72, 487 (1980).
5. N. Inagaki, K. Susuki and K. Nejigaki, *J. Polym. Sci.: Polym. Lett. Ed.*, 21, 353 (1983).
6. E. Kay and M. Hecq, *J. Appl. Phys.*, 55, 370 (1984).
7. M. Hori, T. Yomada, S. Morita and H. Hattori, *Plasma Chem. Plasma Process.*, 7, 155 (1987).
8. L. Maissel in *Handbook of Thin Film Technology*, edited by L. Maissel and R. Glang (McGraw-Hill, N. Y., 1970), Chap. 18.
9. L. Martinu, *Vacuum*, 15, 21 (1987).
10. J. Perrin, B. Despax and E. Kay, *J.*

- Vac. Sci. Technol., A4, 46 (1986).
11. H. Dimigen, H. Hubsch and V. Schaal, Proc. IPAT'85, Munich, p.267.
12. J. W. Coburn and M. Chen, J. Appl. Phys., 51, 3134 (1980).
13. S. F. Durrant, R. P. Mota and M. A. Bica de Moraes, Thin Solid Films, to be published.
14. H. M. Tong and K. L. Saenger, J. Appl. Polym. Sci., 38, 937 (1989).
15. T. Shiosawa and M. A. Bica de Moraes, J. Appl. Phys., 70, 4883 (1991).
16. See for instance: I. Nagai, A. Ishitani and H. Kuroda, J. Appl. Phys., 67, 2890 (1990). J. W. Zou, K. Schmidt, K. Reichelt and B. Dischler, J. Appl. Phys., 68, 1558 (1990).
17. H. Biederman and L. Martinu in *Plasma Deposition, Treatment and Etching of Polymers*, edited by R. d'Agostino (Academic Press, N. Y., 1990), Chap. 4.
18. B. Abeles and J. I. Gittleman, Appl. Opt., 15, 2328 (1976).
19. T. Shiosawa, M. Sc. Thesis, Instituto de Física, UNICAMP, 1991.
20. H. Yasuda, *Plasma Polymerization* (Academic Press, N. Y., 1985), p.337.
21. H. Yasuda, T. Hirotsu and G. Olf, J. Appl. Polym. Sci., 21, 3179 (1977).